



DOI: 10.5281/zenodo.1069529

SEISMIC EVALUATION OF MASONRY MONUMENTS THROUGH THE UTILIZATION OF IN SITU MEASUREMENTS CASE STUDY ON A BYZANTINE BASILICA

Thomas N. Salonikios* and Kostantinos E. Morfidis

Institute of Engineering Seismology & Earthquake Engineering EPPO-ITSAK, P.O. Box 53 Finikas

GR-55102 Thessaloniki, GREECE

Received: 01/06/2017

Accepted: 25/11/2017

**Corresponding author: Thomas N. Salonikios, salonikios@itsak.gr*

ABSTRACT

This study develops an approach to examine parameters that are used for the estimation of seismic loads for historic buildings. A literature review is presented, and data from the literature and laboratory tests are used to assess the provisions that should be satisfied after the restoration of such buildings. In the analysis, frames with nonlinear properties that model stone masonry plain frames are used to estimate the equivalent seismic acceleration that these frames can resist. To investigate the response of masonry monuments to strong earthquakes, the observed response of many temples is considered during seven earthquakes in Greece, and the response spectra are defined for equivalent damping levels of 5%, 10%, and 20%. The aforementioned approaches are used to examine the possibility of further reducing the considered seismic loads for the evaluation of these structures. Alternative methods for the justified reduction of the seismic force by increasing the behavior factor are proposed. Finally a case study is presented on the initial construction stage of a byzantine basilica. In this case, the observed failure of the main roof of the temple and the limitation of damages to the rest of the structure thanks to the use of the findings of the present research is justified.

KEYWORDS: Masonry Monuments, Seismic Loads, Equivalent damping, Behaviour Factor, Earthquakes, Nonlinear response, In-situ Measurements, Post-Event Method

1. INTRODUCTION

Masonry walls were used in many great structures during antiquity, from the early periods until the late Middle Ages period, Fig.1. Impressive historical structures survived along centuries, some of

them with minor damages and many of them with sufficient structural problems. As centuries passed, the construction philosophy of masonry walls was changed and was appropriately adapted, mostly on the basis of trial and error methods.

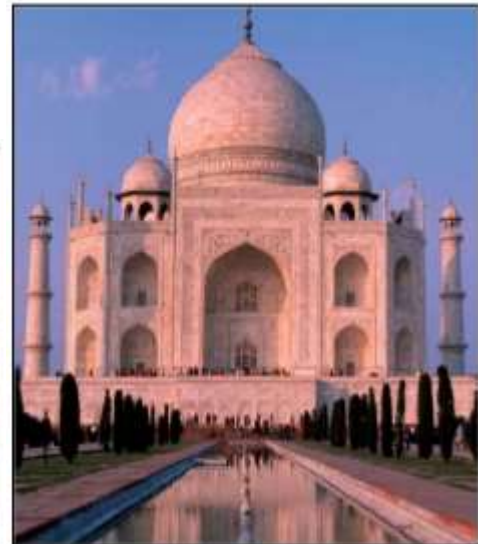


Figure 1. Important masonry monuments

Figure 1 shows historic buildings, with masonry walls, that were successfully conserved and were delivered to humanity in their present form. These monuments need conservation that should be validated through calculation processes. By the use of

these processes, restoration and repair works are scientifically validated in many important monuments. One of the most devastating loads of these structures is earthquake ground motion. Many of the methods used in the seismic evaluation, upgrade

and/or assessment of archaeological masonry monuments were initially established for the design of new multi-story concrete or steel structures. The seismic evaluation of monuments is performed by using methods that are force- or displacement-based and also advanced methods that employ complex calculations with natural and artificial accelerograms. When desirable, advanced software with many capacities may be used to simulate materials, stiffness properties and loads, particularly in the case where these characteristics are documented by in situ tests, thus increasing the provided accuracy (Elyamani et al 2018a,b,c).

Studies focused on the seismic evaluation and restoration of monuments are based on the use of software codes that are widely used by practitioners. In this case, the methodologies and provisions that are applied use: i) low behavior factors ($q=1.0-2.0$), ii) effective accelerations of seismic codes and iii) appropriate acceleration distribution based on the actual masses distribution. In contrast, many cases exist in which the performed restorations are based on the observed and documented response of the monuments to real earthquakes during the period of their existence. The first case is covered by law but, in the second case, the engineer is exposed and not covered by a code that has the validity of a law. In some countries, codes have been established for this purpose, resulting thus to the provision of useful tools for the engineers and coverage by these codes that are laws. In scientific progress, there is always room for improvement. To exemplify, the seismic loads in these codes are calculated using acceleration spectra that resulted from the use of single-degree-of-freedom oscillators that were formed based on the assumption that the mass is largely concentrated at the floor levels. The masses in masonry monuments are typically distributed along the height of the load-bearing walls, whereas the mass is quite low at wooden floor levels. Although many assumptions are contradictory, the restoration of monuments should proceed and thus rational proposals on the aforementioned open issues should be presented on the basis of documented data. These proposals should be combined with appropriate solutions that were determined using the observation of the actual response of masonry monuments to real earthquakes of various intensities.

In the present study, experimental studies related to the examination of masonry wall specimens are reviewed to better approach equivalent damping and to examine the value that was obtained, in comparison with the value that is suggested by the relative codes. Data from laboratory tests are used for the check of the limits that should be considered between the main states of performance. In the analysis

field, frames with nonlinear properties that model masonry plain frames are used to estimate the equivalent seismic acceleration that these frames may resist (in the shape of a capacity curve). The observed responses of masonry monuments in Peloponnesus (in southern Greece) during seven earthquakes are considered, and the damages are correlated to the normalized spectral accelerations for equivalent damping levels of 5%, 10%, and 20%. The aforementioned approaches try to shed light on the exact response of the monument buildings when subjected to strong earthquakes. Afterwards, these outputs and methodologies may be utilized by existing codes or by codes that are under composition for practical use, through appropriate adjustment.

2. LITERATURE REVIEW

The literature review was conducted by searching for ways of using seismic loads with values that will be determined by rational methodologies appropriate for the structural system of masonry monuments. In current methodologies, the procedures employed are documented by the fact that the load carrying walls in historical buildings have generally brittle response, and behavior factors of approximately 1.5 are derived using the available equivalent ductility. Aside from the ductility, criteria for damping also exist. During the evaluation of masonry monuments, the seismic loads are estimated to be reduced by a factor greater than 1.5 due to the available equivalent damping of the structural materials and elements. Equivalent damping, defined as the total viscous and "hysteretic" damping, is significantly greater than 5% when the post-cracking response of the load-bearing masonry walls is considered. In what follows, experimental studies that support this proposal are presented.

According to Beucke and Kelly (1985), the damping in load-bearing masonry walls is composed of viscous damping (ξ) and friction damping. Friction damping is composed of constant Coulomb damping ($x_c.k$) and linear damping ($\zeta.k$) (see Figure 2). These damping components result in the equivalent damping ξ_{eq} :

$$\xi_{eq} = \frac{1}{\pi k \beta x_0} \cdot \{ \pi k \beta x_0 \xi + 2F + \zeta k x_0 \} = \xi + \frac{2x_c}{\pi \beta x_0} + \frac{\zeta}{\pi \beta}$$

The definitions of the symbols are as follows:

ξ : Viscous damping

k : Stiffness of the structure

x_c : Displacement corresponding to the equivalent "yield" of the load-displacement curve. The constant force "F" due to static Coulomb friction is $F = x_c.k \Rightarrow x_c = F/k$

ζ : Coefficient of linear friction (ζk = rate of increment in the damping force due to the displacement).

β : Ratio of the main frequency of the excitation to the eigenfrequency of the structure, i.e., ω / ω_0 .

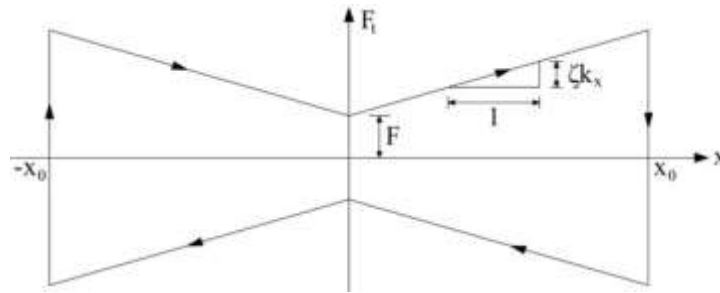


Figure 2. Diagram of friction resistance as a function of displacement (Beucke and Kelly 1985).

The aforementioned equation is a simplified expression of the equivalent damping. This equation closely approaches the exact solution, as was shown by the parametric analyses in this work.

In the study by Calvi, Kingsley and Magenes (1996), masonry specimens were tested pseudodynamically and on a seismic table. Variation in the response with respect to the aspect ratio of these elements was observed during tests on spandrels and piers. In the case of high aspect ratios, a rocking response that is the result of the cyclic bending moments of these elements was observed. Significantly less seismic energy is dissipated in such bending responses than the one dissipated in the shear response. During rocking, the unloading curve follows the path of the loading curve with lower strength, which indicates that a considerable amount of the energy required to achieve the maximum displacement is returned to the building during unloading. From the response observed during the diagonal tension cracking of specimens, the unloading path follows a nearly straight line, thus enlarging the area of the hysteresis loops. This research found that, during the sliding shear response of masonry specimens, a higher percentage of the input seismic energy is dissipated compared to the rocking and diagonal shear mechanisms. The disadvantage in the case of the sliding shear response is the existence of higher permanent deformation. Rocking and sliding shear responses can occur simultaneously due to the reduction of the portion of the section that is under compression in the case of the rocking response. The response to diagonal compression is typically quite brittle due to the eruptive type of this cracking. Under the appropriate conditions (aspect ratio less than 1.0), the response of masonry walls to diagonal tension is "ductile" and is developed more significantly by the failure of mortar joints than by the failure of bricks. In these cases, the response of the specimen after cracking is not considered as destructive, and a significant capacity for vertical load carrying remains. In vibration tests of a monument specimen at the natural scale, an approximately 50% reduction in

the main eigenfrequencies of the specimen was observed.

Magenes and Calvi (1997) presented an equation for the shear strengths that correspond to rocking, diagonal shear and sliding shear responses. Estimation of the dissipated seismic energy input to these mechanisms was also discussed. During the rocking (flexural) response of masonry piers, the equivalent ("hysteretic" and viscous) damping is approximately 15%. Similarly, during the diagonal tension response, the equivalent damping is 20%. This value is considered to be conservative. For the sliding shear response, the authors provided an equivalent damping of 64% at the level of high displacement. The sliding shear response always appears together with rocking and diagonal tension. For this reason, consideration of such high equivalent damping is not realistic. Until 1997, few significant experimental results were available concerning the contribution of the sliding shear response to the absorption of seismic energy during the development of the mixed failure mode. An equivalent damping of 15% and an ultimate 1.0% drift for rocking response were suggested when simulating the piers and spandrels of a masonry structure with linear elements. For diagonal tension cracking and the sliding shear response, equivalent dampings of 15% and 20% and ultimate drifts of 0.5% and 1.0% are respectively suggested (the value of 20% for equivalent damping is considered to be conservative). The failure modes for flexural, diagonal tension and sliding shear are defined by simplified equations in the work of Magenes and Calvi (1997). By the use of these dampings, the reduction to the spectrum of Eurocode 8 is approximately 1.80. This reduction is greater when the response spectra of actual earthquake recordings are used. The results indicated that a behavior factor of 1.5 is highly conservative and that higher values are obtained if the entire building is modeled, due to the combined contribution of post-elastic mechanisms, equivalent damping and a change in the eigenperiods of the structure.

Tomazevic and Weiss (1994) presented results obtained from the seismic table testing of a masonry monument model that was constructed at a 1:5 scale. An approximate 40% reduction in the main eigenfrequencies was observed during the tests. The energy "E" (hysteretic and input energy quantities) ratio of E_{hys}/E_{inp} was 50% for the unreinforced (hysteretic and input energy quantities) masonry building model, for displacement $d/d_{top} > 0.5$. A behavior factor of $q=2.84$ was obtained from the tests on the masonry monument. The value proposed by Eurocode is conservative but appears reasonable in the case in which it is necessary to avoid damage to masonry monuments.

Bothara et al. (2010) presented results from seismic table tests of a masonry building that was constructed on a 1:2 scale. The building was subjected to seismic excitations in two directions. The percentages of dissipated energy for various levels of displacement and the correlating vulnerability were calculated on the basis of these tests, and the results indicated that the energy-effective damping percentage during the tests was 36% (Table 1). This result demonstrates a significant capacity of masonry monuments for steady nonlinear response when they are subjected to strong seismic excitations. This observation is attributed to either rocking or the reduction of the eigenfrequency of the building (softening) due to the cracking in shear mechanisms.

Table 1. Characteristics of the response of a building model tested on a seismic table (Bothara et al. 2010)

Boundary	Drift limit (%)	Δ_{Model} (mm)	$\zeta_{effective}$ (%)	B_{ζ}	$\Delta_{Prototype}$ (mm)	Expected PGA (g)
<i>Color code</i>						
Green-yellow	0.1	2	20	1.58	4	0.35
Yellow-orange	0.4	8	33	1.95	16	0.43
Orange-red	0.8	16	35	2.00	32	0.53
<i>Damage state</i>						
1-2	0.1	2	20	1.58	4	0.35
2-3	0.5	10	34	1.97	20	0.43
3-4	0.9	18	35	2.00	36	0.56
4-5	1.3	26	36	2.02	52	0.69

In the work by Ahmad et al. (2010), the energy dissipated in masonry structures subjected to strong earthquakes was related to the achieved ductility using the equation $\xi=0.05+c(\mu-1)/(\pi\mu)$. The coefficient c was estimated based on experimental results on masonry pier specimens and was found to have a value $c=0.32$.

Michel et al. (2011) estimated the percentage decrease in the fundamental eigenperiod of masonry structures relative to the drift achieved on the walls of these structures. The results obtained from a test at the ELSA laboratory at Ispira in Italy were presented. More specific results were provided on the basis of two tests on natural-scale building models that were tested pseudo-dynamically. One building model was constructed using clay bricks and the other was constructed with limestone bricks. These tests yielded the relation between the reduction in the eigenperiod of these buildings and the factor that converts the vertical loads to a seismic horizontal load (%g).

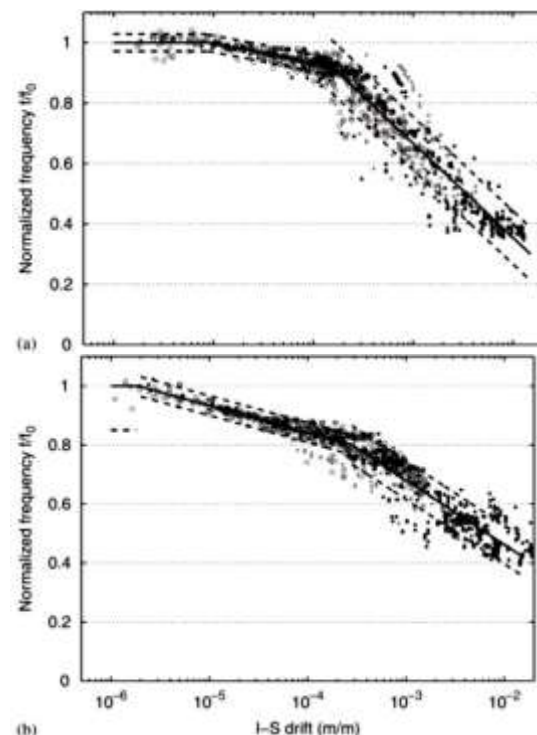


Figure 3. Reduction in the main eigenfrequency of the tested buildings relative to the achieved "I-S (inter-story) drift" for (a) limestone bricks and (b) clay bricks. White dots=2-10%, gray dots=12-14%, black dots>16%g. Trilinear approach of the data (continuous line) and 80% confidence interval (discontinuous lines) (Michel et al. 2011).

The numerical approach for the aforementioned diagrams (Figure 3) is given by the following equations:

$$\begin{aligned} D \leq D_0, & \quad f/f_0 = 1 \\ D_0 < D \leq D_1, & \quad f/f_0 = 1 - \alpha_1 \log(D/D_0) \\ D_1 \leq D, & \quad f/f_0 = (1 - \alpha_1 \log(D/D_0))(1 - \alpha_2 \log(D/D_1)) \end{aligned}$$

The initial branch is horizontal, the second branch has a slope of α_1 , and the third branch has a slope of α_2 . The drift at the first point where the first and second branches intersect is D_0 , and the drift at the intersection point of the second and third branches is D_1 . The main eigenfrequency of the structure is f_0 . In the first branch, the eigenfrequency is not altered for an inter-story drift D_0 of 8.7×10^{-6} or 1.8×10^{-6} for limestone or clay bricks, respectively. This area is considered as the area of weak ambient vibrations. For drifts greater than D_0 , the eigenfrequency is slightly reduced without significant damage. The inclination α_1 is -0.027 for the building with lime-

stone bricks and -0.040 for the building with clay bricks. After point D_1 with an inter-story drift of 0.015% for limestone bricks and 0.028% for clay bricks, the eigenfrequency decreases more rapidly. The inclination α_2 is -0.135 in the first case, but -0.095 in the second case. At the failure inter-story drift of 0.5%, the eigenfrequency is reduced between 0.5 to 0.4 of the initial value. For an inter-story drift of 0.1%, which is the typical level of deformation and corresponds to crack initiation, the reduction is $0.67 \pm 9\%$ of the initial eigenfrequency. In practical terms, at the equivalent yield point, a reduction in the eigenfrequency by 2/3 of the elastic value could be considered. This reduction corresponds to a stiffness reduction of 50%. The main objective of the aforementioned models with reduction of the main eigenperiod is the better estimation in the seismic evaluation of the masonry monument and the definition of the subsequent damages. Table 2 suggests that failure occurs for a seismic coefficient of 0.2g, which is significantly lower than the ordinary values obtained by the use of evaluation codes.

Table 2. Reduction in the main eigenfrequencies of the tested buildings relative to the seismic coefficient (%g) (Michel et al. (2011))

Tests (% g)	0.02	0.04	0.06	0.08	0.10	0.12	0.14	0.16	0.18	0.20	0.22
Clay (Hz)	6.1	5.9	5.7	5.5	5.2	5.0	4.45	4.1	4.0	3.6	3.1
Calcium silicate (Hz)	6.3	6.2	6.25	6.0	5.8	5.6	4.3	4.45	4.15	3.4	-

In summary, compared to new constructed masonry monuments, existing monuments that were constructed during past centuries with empirical techniques and mortars of lower strength display a higher damping capacity (viscous and hysteretic), a lower stiffness, a higher capacity for seismic energy dissipation, and a higher displacement capacity. The aforementioned conclusion is obtained by considering the additive strain on load bearing walls due to accumulative deformations at the foundation level, the formation of various types of cracks at the walls during centuries, the loosening of connections during the various loading cycles (vertical live loads, wind and earthquake loading) and material aging. This actual response, in comparison with the findings from the literature review, show that the masonry walls of historic building exhibit a capacity for "equivalent hysteretic" response that needs to be modelled and quantified for use in research and practice studies. This is attempted in the following chapters.

3. USE OF EXPERIMENTAL DATA TO VALIDATE THE CODE PROVISIONS

In the current section, results are given from experimental studies on masonry specimens to better understand the shear strength of masonry walls and

estimate the available deformation capacity are used. The load - deformation laws of masonry specimens tested at the laboratory are presented in order to understand the available deformation capacity of masonry walls. The specimens used were obtained from experimental studies conducted by Magenes and Calvi (1997), Abrams (1992), Abrams and Shah (1992), Da Porto et al. (2009), Tomazevic (2009), Coradi et al. (2002), and Ignatakis and Stylianidis (2004). The flexural and shear strengths were calculated for these specimens and in 85% of the specimens, the shear strength was less than the shear that corresponds to flexural failure. In Eurocode 8-3 (2005), the design shear strength of the specimens should not be greater than 6.5% of the compressive strength of the masonry wall f_m ($f_{vd} \leq 0.065f_m$) whereas, in Eurocode 6 (2005), this inequality is $f_{vd} \leq 0.065f_b$, where f_b is the strength of the brick. The resulting compressive strengths differ considerably. Such differences could be eliminated by the appropriate choice of D' (the length of the portion of the cross-section that is under compression). For this reason, the use of $D'=D$ is suggested in the first inequality and the use of $D'=0.4D$ is suggested in the second inequality. The aforementioned checks are shown in Figure 4. The experimental strengths are shown in comparison with the calculated values. In the case of

the seismic evaluation of existing monuments, the engineers should be covered by a code that should have been accepted by the governmental bodies as a national law. This is not happening in many modern

countries. For this reason, engineers may use the most relevant code for the seismic evaluation of masonry monuments i.e. Eurocode 8-3, Eurocode 6, in order to be covered by an approved code.

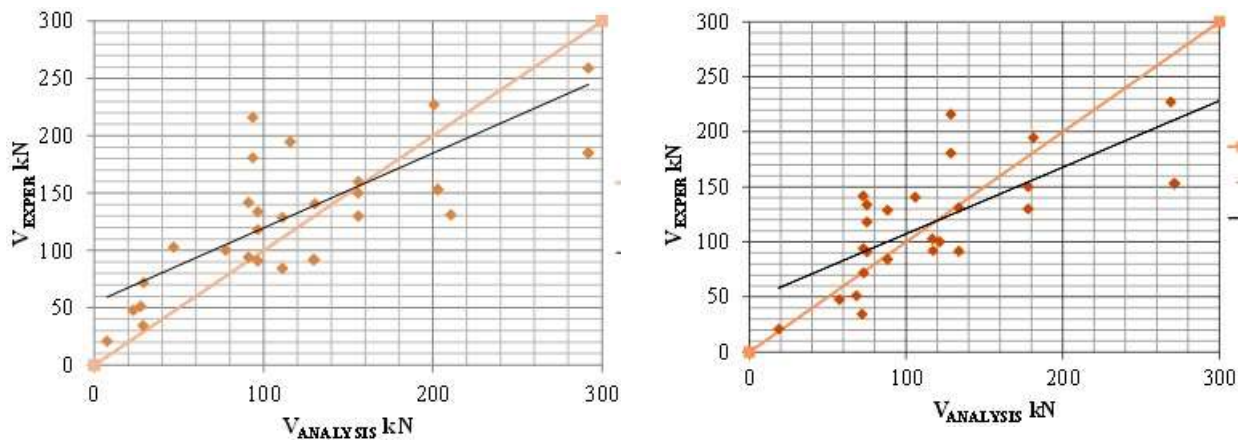


Figure 4. Comparative diagram for the experimental V_{EXPER} and shear strengths of the considered masonry specimens; for: Left $D'=0.4D$ and $f_{vd} \leq 0.065f_b$, Right $D'=D$ and $f_{vd} \leq 0.065f_m$. $V_{ANALYSIS} = f_{vd} \cdot D' \cdot t$

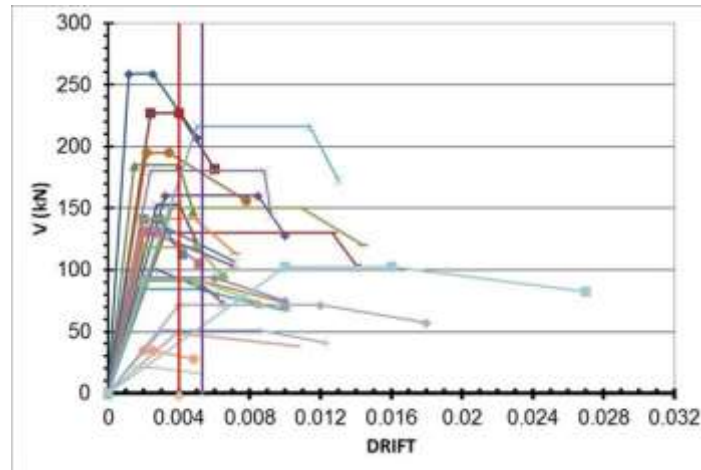


Figure 5. Load-drift envelope curves for the considered specimens. Limits between states: damage limitation (0-4‰), significant damage (4-5.3‰) and near collapse (>5.3‰). Horizontal axis represents the ratio of horizontal displacement of the specimen (δ) divided by its height (H), $DRIFT = \delta/H$.

Figure 5 presents the three points that define the tri-linear envelope curve of the load-drift curve for the considered specimens. The ascending branch is defined by the zero point located at the beginning of the axis and the curve point located at $0.8V_{max}$. This branch intersects the horizontal line defined by the maximum strength of the specimens. The descending branch connects the point of maximum strength with the 80% strength reduction point of the behavior law curve for the specimens. An equivalent yield point can be defined at a drift ratio of 2.0‰. In this case, it is possible to develop an equivalent ductility capacity for the masonry wall of approximately $\mu_{mid,eq} = 5.3/2.0 = 2.6$. The aforementioned comparisons shows that the masonry walls are not quite brittle when subjected to seismic loads. In some cases, the equivalent ductility factor is higher than the medium

ductility value, thus indicating that there are inelastic deformation reserves that are quantified in Figure 5.

4. INELASTIC ANALYSIS OF MASONRY PLANE FRAMES

Next, masonry plain frame analyses are used to define the equivalent seismic coefficient as a percentage of the vertical loads of these frames. This coefficient is defined by considering the force that these frames can resist. The applied load was a one-directional horizontal load that was increased by a predefined load step. These analyses were performed with consideration of nonlinear material properties, element stiffness and loads according the typical values that are observed in ordinary masonry monuments in Greece and were presented in detail by Salonikios et al. (2003). In the framework of the

current study, these analyses are presented in Figures 6 and 7 so as to define the seismic coefficients that may be resisted and to relate these coefficients to the seismic accelerations. Table 3 illustrates that a higher strength is obtained in the case of continuous element models than that in the case of discrete brick-mortar joint element models when masonry plain frames are modeled. In addition, the strength obtained when the seismic loads are distributed along the height of the frames relative to the distri-

bution of the mass along the height (ACC) is greater than that in the case in which the seismic loads are distributed in an inverted triangular mode (LOAD) or relative to the shape of the main mode (MODE). For the considered plain frames with discrete brick-joint elements and with properties of ordinary masonry monuments (masonry compressive strength of 2.5-3.0MPa), the seismic coefficient that can be resisted is approximately 0.26 g.

Table 3. Seismic coefficients for various types of nonlinear masonry frames and various seismic load distributions.

FRAME TYPE	"Equivalent" seismic coefficients			
	1 BAY		7 BAY	
	LOAD/MODE	ACC	LOAD/MODE	ACC
SAP2000 Nonlinear Frame Elements	0.26 g		0.24 g	
Continuous Model	0.30 g	0.36 g	0.47 g	0.55 g
Discrete Model	0.25 g	0.31 g	0.29 g	0.33 g

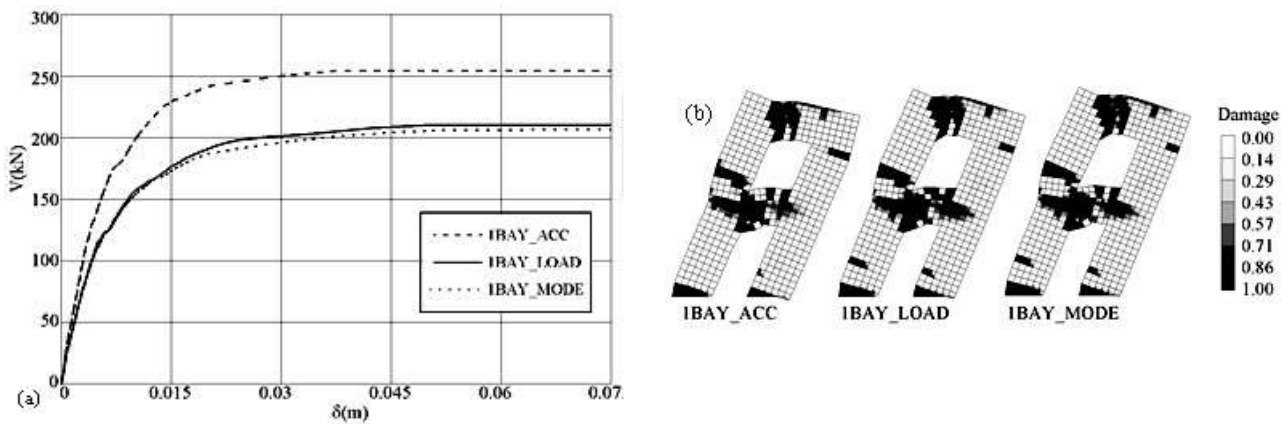


Figure 6. (a) Load-deformation curves for two-story, one-bay masonry frames with continuous finite elements, (b) damage types

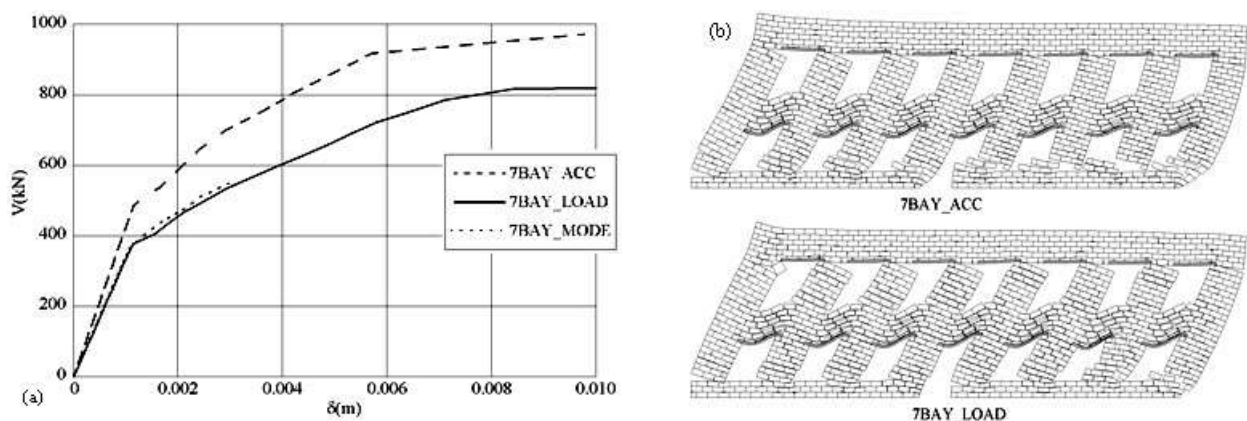


Figure 7. (a) Load-deformation curves for two-story, seven-bay masonry frames with discrete finite elements, (b) failure types

5. USE OF RECENT SEISMIC EVENTS TO VALIDATE THE MASONRY MONUMENT RESPONSE

This section presents the results obtained from the post-processing of strong seismic events recorded by the National Strong Motion Network of IITSAK-EPPO. These earthquakes occurred in Peloponnesus, in southern Greece. Immediately after these earthquakes, in situ inspections were performed to observe the response and damage to masonry monuments. More specifically, the earthquakes of Kalamata (1986), Aegion(1995), Pyrgos (1993), Kythera(2006), Leonidio(2008), Koroni (2008), Vartholomio(2002) and Achaia-Ilia(2008) were selected. In the response spectra of these earthquakes, the level of normalized (0.66 of the maximum) spectral acceleration was determined for damping levels of 5%, 10% and 20%. Furthermore, the response of the masonry monuments for these earthquakes is described.

5.1. Kalamata Earthquake (1986, M6.0)

This earthquake occurred at a low depth of 8 km, and the epicenter was located approximately 12 km from the town center (Karantoni and Fardis 1992, Theodulidis et al 2004). Masonry monuments in Kalamata typically consist of two stories and a basement that is commonly located partially above ground. Exterior load-bearing walls with a thickness of approximately 0.6 m are typically made of plastered rubble-stone masonry but may also consist of solid or hollow bricks, or a combination of all three. Horizontal steelties connecting transverse load-bearing walls are common but are typically corroded. Both stories typically feature light wood floors on

timber joists that are weakly anchored to the exterior walls in the direction of the joists. Floors often rest on interior load-bearing walls extending up to the second-story floor. Buildings are covered by hip or gable roofs consisting of wood truss framing and clay tiles nailed to wood sheathing. This type of construction for monuments is common in all old urban nuclei that have developed in Peloponnesus. Both piers and spandrels are present on the façades of stone masonry monuments. The main types of observed damage are described as follows:

- Diagonal tension cracking in the piers in one or both stories at an inclination to the horizontal that typically exceeds 45°. If windowsills are integral with the adjacent piers, diagonal cracking often extends into the heavy spandrels.
- Vertical cracking of spandrels over the window or door heads, mainly in the top story.
- Separation of the walls from the transverse walls along a nearly vertical line at the corner pier of the second story.
- Out-of-plane collapse of the second-story wall or of the upper portion of the wall.

Wall damage was typically heavier on the second story. An attempt to correlate the damage in a representative sample of 36 two-story monuments with a set of 20 geometric indices considered as descriptive of the structural geometry indicated no statistically significant effect of these geometric indices on the vulnerability of the individual walls or stories of the entire building. This result is attributed to the absence of rigid floor diaphragms that enforce system action, the approximate proportionality between inertial forces and the strength of the walls due to the concentration of building mass at those locations.

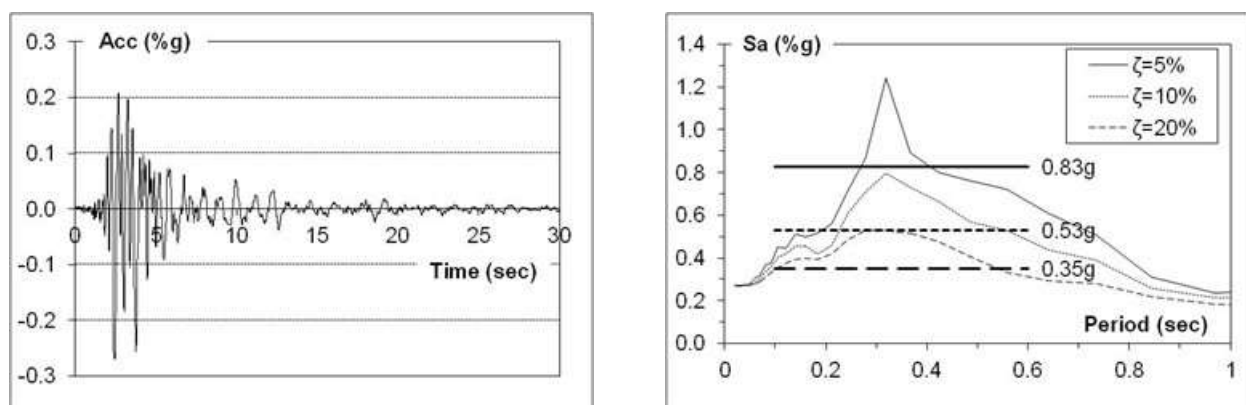


Figure 8. Recorded accelerogram and response spectrum for the Kalamata earthquake ($M_w=6.0$) normalized (0.67 of the maximum value) at damping levels of 5%, 10% and 20%.

5.2. Pyrgos Earthquake (1993, M5.5)

Damage to the masonry monuments was severe, and several of them had to be demolished (Karanto-

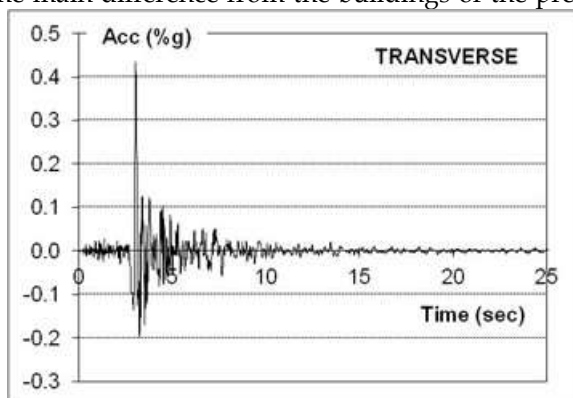
ni and Bouckovalas 1997, Theodulidis et al 2004). These monuments were often one or two stories in height, and the construction materials were adobe,

stone masonry and brick masonry. Monuments constructed from 1800 to 1850 had walls made from handmade air-dried blocks of clay and earth reinforced with hay or straw. These monuments were 1- or 2-story buildings with timber roofs and floors. The damage observed in the load-bearing walls of this type of building included the following: a) vertical cracking in spandrels over openings that are more severe in the upper story, b) turnover of the external layer at the top of the walls and even of the entire wall due to out-of-plane seismic action, and c) local buckling of the lower portions of the walls.

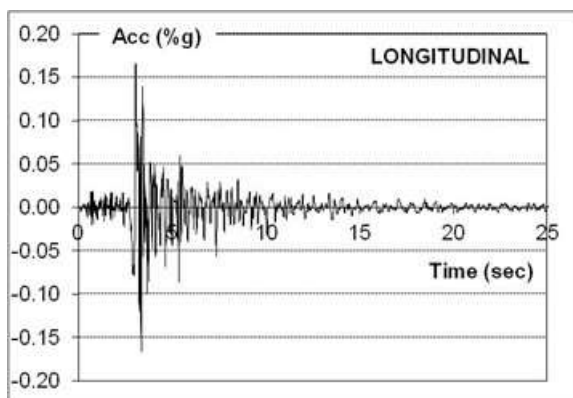
Monuments constructed from 1850 to 1900 primarily contained stone masonry walls with thicknesses of 0.55 to 1.00 m. The floors and roofs are of the same type as in the buildings of the previous category. The most common types of damage for this type of building are as follows: a) vertical cracking of the spandrel of the upper floor and of the corners due to separation of orthogonal walls and b) diagonal cracking of the piers. Diagonal cracks at the first-story piers typically continue throughout the strong spandrel and extend up to the upper story and even to the roof level.

The 1900-1940 monuments were built of stone masonry and a subset consisted of solid brick masonry. The main difference from the buildings of the previ-

ous period was that the windowsills were made from 0.15-m-thick walls acting as infill to the adjacent piers rather than spandrels. The height of the spandrel is formed by the head of the window or door up to the floor of the next story. In this case, it is easier to distinguish between piers and spandrels. The cracking pattern in all of these spandrels is nearly vertical, as in the upper floor. The sills are often separated from the adjacent walls due to the lack of bonding. In addition, the cracks at the ground floor piers do not continue up to the pier of the upper story. When the buildings were damaged at the upper storey, the damage was light and was caused by out-of-plane seismic action. In contrast, when the first story was damaged, the damage was heavy with wide, diagonal cracks and decomposition of the masonry. This damage is due to the in-plane seismic action and occurs in a low percentage of load-bearing piers parallel to the direction of seismic action. Masonry monuments with reinforced floors, roofs and tie beams did not suffer significant damage. For this earthquake, both horizontal components due to the different shape of the response spectrum in each direction were taken into account. The normalized spectral acceleration for 20% damping significantly differs in each direction.



Accelerogram and response spectrum for the Pyrgos Earthquake, 1993, Mw=5.5, Trans. Direction



Accelerogram and response spectrum for the Pyrgos Earthquake, 1993, Mw=5.5, Long. Direction

Figure 9. Recorded accelerogram and response spectra for the Pyrgos earthquake normalized (0.67 of the maximum value) at damping levels of 5%, 10% and 20%.

5.3. Aegion Earthquake (1995, Mw=6.1)

This earthquake was a near-field example. The information given herein was collected by studying the masonry monuments in the central and older areas of the town of Aegion (Karantoni and Fardis 2005, Theodulidis et al 2004). The damage to these buildings in the historical center of the town was rather severe. The most significant damage to masonry monuments in the study area was the flexural damage of the spandrels due to the component of the seismic action transverse to the wall. This caused nearly vertical cracks at the upper corners of the openings and, in the majority of cases, the out-of-plane collapse of walls, the shear (diagonal) failure of piers and the vertical separation of orthogonal walls that resulted in the overturning of the wall, in some cases. One-story monuments with clay brick masonry did not develop shear failure, separation of orthogonal walls or collapse, and only one such building developed cracking of the spandrels and moderate damage. Adobe and stone masonry monuments displayed shear failure, flexural damage in the spandrels and separation of orthogonal walls. The percentage of adobe masonry monuments ex-

hibiting damage was twice that of the stone masonry monuments.

Shear failure of piers was observed at the ground story of two-story monuments. This failure was accompanied by other types of severe damage, largely in adobe and brick masonry monuments and, to a lesser extent, in stone masonry monuments. Cracks due to bending also formed to a large extent in adobe and brick masonry monuments, but to a lesser extent in stone masonry monuments. Damage was observed at the top floor of two-story buildings due to crack development at the spandrels and shear cracking of the piers at this floor. The damage was heavier in adobe and stone masonry monuments and moderate in clay brick masonry monuments.

The following conclusions can be drawn: a) one of the features that affects the seismic performance of masonry monuments and damage is the number of stories (increased damage), b) the damage decreases with increasing masonry material strength, c) the rigid diaphragms reduce the damage, d) the damage in buildings is higher in the upper story and e) older buildings with poor-quality masonry are more vulnerable.

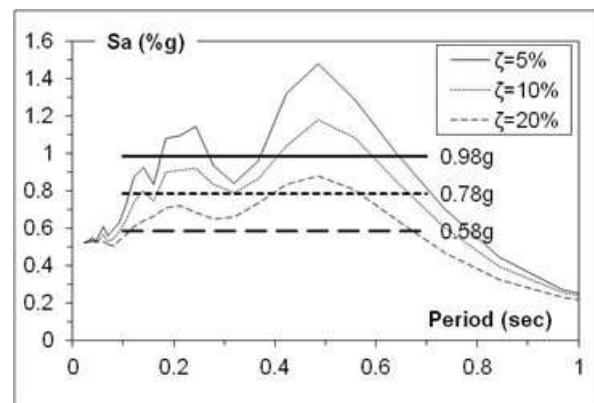
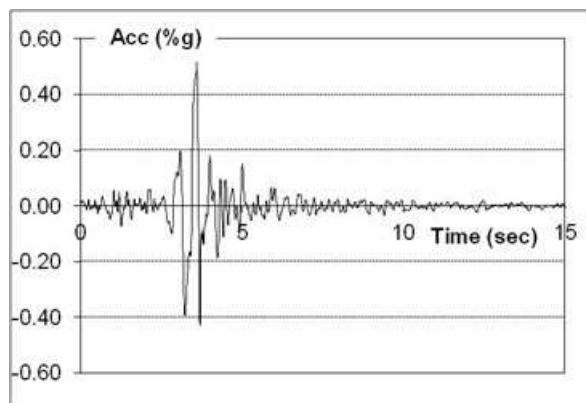


Figure 10. Recorded accelerogram and response spectrum for the Aegion earthquake ($M_w=6.1$) normalized (0.67 of the maximum value) at damping levels of 5%, 10% and 20%.

5.4. Vartholomio Earthquake (2002, M5.6)

The masonry monuments in Vartholomio are typically one- to two-story buildings with a rectangular plan and a symmetrical frame arrangement (ITSAK & IG of NOA 2003). These buildings largely consist of stone masonry monuments with small openings. Wooden friezes are used in the middle of the walls and at the lintels. The masonry walls are typically constructed with the use of low-thickness mortar

joints. These buildings behaved well during the 2002 earthquake. Damage was observed in monuments with larger openings and low-thickness piers. In this case, the ability to resist seismic forces was rather low. The damage developed at the spandrels of the first floor. The damaged monuments were characterized on a scale with three damage levels (green: no or light damage; yellow: moderate damage and red: significant damage).

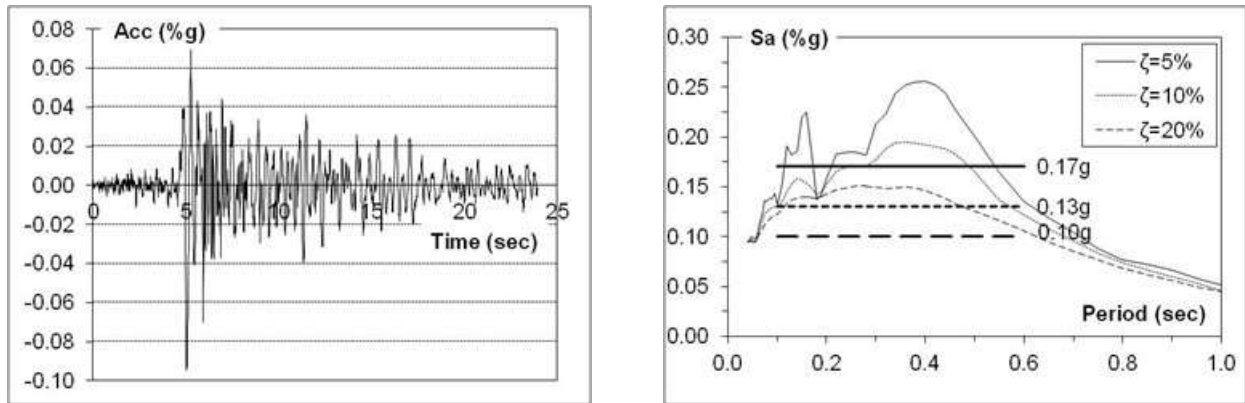


Figure 11. Recorded accelerogram and response spectrum for the Vartholomio earthquake ($M_w=5.6$) normalized (0.67 of the maximum value) at damping levels of 5%, 10% and 20%.

5.5. Kythira Earthquake (2006, M6.9)

The epicenter of this earthquake was located in the sea at a distance of 25 km from the island of Kithira (Karakostas et al., 2006). This earthquake was of intermediate depth (66 km). Traditional stone masonry monuments typically have up to two (and seldom three) stories and constitute a large percentage of the building stock in Kythira. The damage observed in such buildings (mainly cracks and partial collapse of stone walls) should be attributed to a lack of sufficient seismic resistance, as well as to their already poor condition (old age, inadequate maintenance) prior to the main event. Damage to stone masonry monuments was particularly severe in the village of Mitata. The local soil conditions at the site, combined with the age and poor condition of many buildings, might have played an important role in the damage observed. Monuments on the island from the Byzantine era and later suffered the most

serious damage. Many churches were built with stone masonry walls and cracks were observed in several of them, as well as in masonry arches and domes that constitute portions of the structural system. Partial or more severe damage was also observed in several bell towers, which was often due to height and stiffness differences with the main church building to which they were attached. Less severe damage was also observed in several other churches throughout the island, namely in Agios Georgios in the village of Mitata, Panagia Mirtidiotissa in the village of Mirtidia, Agioi Anargyroi in the village of Potamos, Osios Theodoros near the village of Potamos and Timiou Prodromou near the village of Gerakari. The Venetian castle in the town of Kythira, the capital bearing the name of the island, suffered no damage to its exterior walls. Similarly, no damage was reported for the various churches and other masonry monuments in the enclosure of this town.

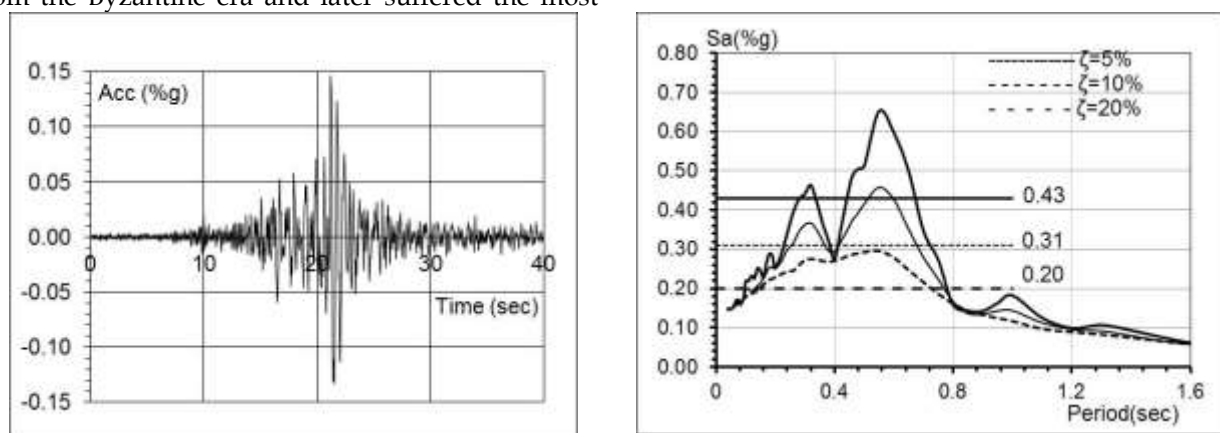


Figure 12. Recorded accelerogram and response spectrum for the Kithira earthquake ($M_w=6.9$) normalized (0.67 of the maximum value) at damping levels of 5%, 10% and 20%.

5.6. Koroni Earthquake (2008, M6.7)

The epicenter of this earthquake is located in the sea at a distance of 30 km from the built environment where the earthquake was recorded and the

response of the masonry monuments was observed (ITSAK, 2008). Many one- to two-story monuments are located in this area. The majority of the damaged monuments are located in Koroni, and the maximum intensity of the earthquake is V+ on the

Mercalli scale. The damage to monuments is largely characterized as light on a scale with three damage

levels (green: no or light damage; yellow: moderate damage and red: significant damage).

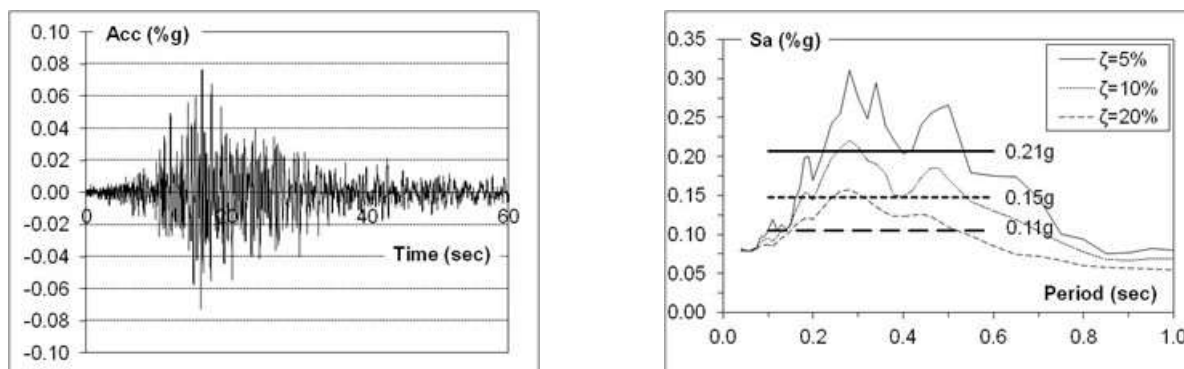


Figure 13. Recorded accelerogram and response spectrum for the Koroni earthquake ($M_w=6.7$) normalized (0.67 of the maximum value) at damping levels of 5%, 10% and 20%.

5.7. Achaia-Ilia Earthquake (2008, $M6.5$)

Masonry monumental buildings in the area typically contained one to two stories (ITSAK, 2008). These buildings are brick masonry monuments of cultural importance and constitute a special subcategory, as described in further detail below. Damage (cracking and collapse of stone/brick/mudbrick walls) in these buildings can be primarily attributed to insufficient or non-existent seismic resistance measures, as well as to their already poor condition (old age, inadequate maintenance) even before the earthquake. The most extensive failure in the masonry monumental buildings was observed in masonry churches and their bell towers. The majority of churches in the area have stone masonry exterior walls with an orthogonal plan. Cracking was observed on the exterior walls (mainly near window and door openings), as well as at the junctions of the exterior walls. Damage to masonry bell towers was also observed at the height above which the tower protrudes from the adjacent main building or in the columns at the bell level, where large openings are

found. In several cases of masonry monuments of cultural heritage, damage was mainly concentrated around openings or at the top of the exterior walls on which (typically) wood roofs rest. In the town of Amaliada, severe cracks were observed in several interior masonry arches in the main church building. The exterior walls of the church were strengthened (at their exterior face) in 1995-1996 with gunite and did not exhibit any damage. Brick masonry residential buildings of cultural importance fall within the same category. The majority of these buildings were either renovated or in a better state of maintenance than the remainder of the common masonry monuments of the area and hence presented better seismic behavior overall. In these buildings, the observed damage consisted primarily of cracking at the upper portions of the load-bearing walls or at piers and spandrels formed by the window and door openings. The in situ inspections indicated that brick masonry monuments of cultural importance generally suffered less damage due to their good maintenance conditions.

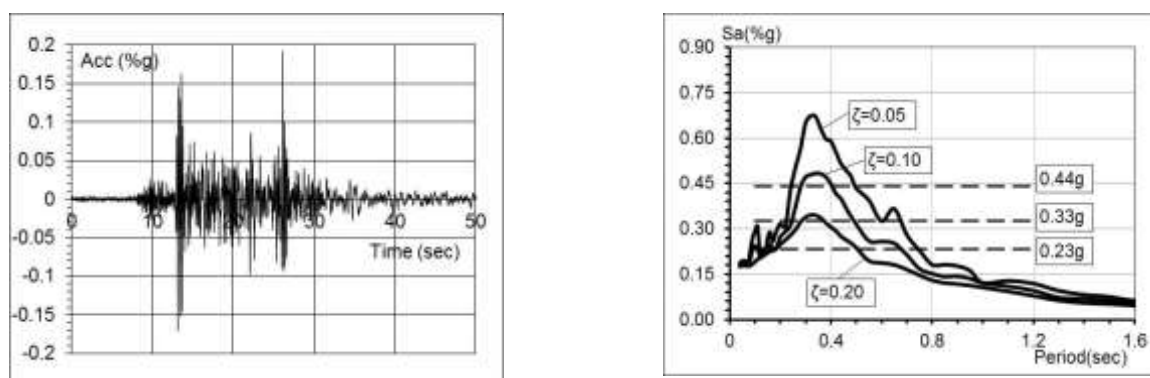


Figure 14. Recorded accelerogram and response spectrum for the Achaia-Ilia earthquake ($M_w=6.5$) normalized (0.67 of the maximum value) at damping levels of 5%, 10% and 20%.

Table 4. PGAs and spectral accelerations for various damping ratios for the recorded earthquakes (Data from figures 8-14).

	PGA	5% Sa (n=0.67)	10% Sa (n=0.67)	20% Sa (n=0.67)	Monument Damage Rank
Kalamata Earthquake	0.27 g	0.83 g	0.53 g	0.35 g	Serious
Pyrgos Earthquake	0.43 g	0.56 g	0.51 g	0.44 g	Serious
Aegion Earthquake	0.51 g	0.98 g	0.78 g	0.58 g	Serious
Vartholomio Earthquake	0.10 g	0.17 g	0.13 g	0.10 g	Light or Non
Kythera Earthquake	0.15 g	0.43 g	0.31 g	0.20 g	Light
Koroni Earthquake	0.08 g	0.21 g	0.15 g	0.11 g	Light or Non
Achaia-Ilia Earthquake	0.16 g	0.44 g	0.33 g	0.23 g	Moderate

Table 4 illustrates that when spectral acceleration that corresponds to 5% damping is applied to evaluate the monuments of the stricken area, these monuments are analytically collapsed due to the high value of acceleration. When using spectral accelerations that result from considering an equivalent damping of 20%, the extracted conclusions reflect the damage situation of the area monuments more efficiently. Considering this damping ratio results in an average reduction factor to seismic loads of 2.0. Another important observation from this portion of the calculation is that when considering 20% damping, the block response is attributed to the structural systems of the monuments. This result is justified by considering the drifts in Figure 5, which are significantly low. In the case of initiation/formation of the first cracks, i.e. the checkpoint for force-based design, the corresponding drift is 2‰, resulting in a nearly box-like behavior.

6. DECISION OF INTERVENTION SCHEME THROUGH IN SITU MEASUREMENTS

In this chapter, a methodology is provided that contributes to the decision making for the restoration of monuments. The method is called «After Event Method». Through the use of this method, it is possible to make rational decisions for the level of restoration that should be applied to the structural elements of any monument for which structural upgrade and/or conservation must be determined after a destructive earthquake. The analytical model of a monument can approximately replicate the original response and determine a basis for strengthening and increasing the deformation capacity of the structure to the levels defined by national codes or decision-making bodies. This methodology is schematically illustrated in Figure 15. In this figure, the use of high sensitivity sensors for the measurement of response of the monument to ambient or stronger vibrations is prescribed. The measurement points should be defined according to the targets of the

study. In case it is desirable to test the effectiveness of the interventions to provide diaphragmatic action, the sensors should measure at the locations along the main walls and colonnades, as well as at the vertical direction. The resulted eigenperiod from the measurements at the vertical direction at the middle of the walls should be the same with the eigenperiod that resulted from measurements along the walls that are parallel with the aforementioned direction.

The literature review suggests that many reasons exist for the consideration of a significant “equivalent hysteretic” response in a masonry monument. Seismic evaluation of masonry monuments is typically performed for a predefined deformation and damage level. At these levels, a significant capacity for dissipation of the input seismic energy ensues. The dissipation is attributed to the equivalent viscous and “hysteretic” response with a total value of approximately 20%. In addition, another important parameter for the definition of seismic loads is the reduction of the eigenfrequency of masonry monuments when subjected to strong earthquakes. For drift ratios over 0.1% up to a level of 0.5%, the obtained reduction in the main eigenfrequency is 67% and 50%, respectively. The seismic coefficient in this case displays a maximum value of 20%g. In these cases, the stiffness of the structure should be reduced by at least 50%, resulting in the development of significantly lower section forces on masonry elements, compared to the case in which the elastic stiffness is considered. The review of the literature tests and Eurocode 8 Part 3 provisions suggests that 5.3‰ is a reasonable value for a failure drift. These values of behavior factors or the equivalent reduction in seismic loads are justified by considering the limits that are defined in Eurocode 8 Part 3. More specifically, the diagram in Figure 5 illustrates that the near-collapse drift level is approximately 5.3‰. In addition, the same data indicate that 2.0‰ is a reasonable value for the equivalent yield drift, resulting in an equivalent ductility of 2.6. In this case, the derived

behavior factors are greater than 1.5 and closer to a value of 2.0. It is generally accepted that masonry walls have a low capacity for ductile behavior and absorption of the seismic energy that is inserted into masonry monuments. For these reasons, the designed seismic loads are reduced to a significantly lower extent than the seismic loads that are considered in the design of reinforced concrete and steel structures. In the current study, a distinction is made for "experimental works" for which it was proven that masonry walls might normally develop an equivalent damping of 20% and an equivalent ductility of approximately 2.6g. The considered strong earthquakes in Peloponnesus occurred in locations with a seismic zone characterization of II and an effective acceleration of 0.24g. In this case, masonry monuments should be examined for evaluation accelerations of 0.4g when a behavior factor of 1.5 is considered. Examination of the reduction that can be achieved when an equivalent damping of 20% is considered demonstrates that seismic loads might be reduced by a factor of 2.0. This reduction in the seismic loads is greater when the equivalent ductility is considered for load-bearing masonry walls. A generally higher reduction factor is justified by considering the earthquakes that were recorded in Peloponnesus by the National Strong Motion Network of Greece. Additionally, in the framework of the current study, an evaluation methodology is presented for application to cases in which a decision regarding the restoration or strengthening of a monument is required. It is possible to estimate the initial stiffness and eigenproperty conditions of a damaged monument for a rational decision in the intervention scheme. In this case, one might select restoration or strengthening or both strength and deformation capacity increments through the use of a calibrated analytical model.

7. CASE STUDY ON THE INITIAL CONSTRUCTION PHASE OF A BYZANTINE BASILICA

Panayia Acheiropoietos (Figure 16), is a typical example of an early Christian three-aisled timber roofed basilica with narthex and galleries. The building is 51.90 m long, 30.80 m wide and 14 m high at

the side external walls, and 22 m high at the top of the roof of the central aisle. This structure was originally larger than it is today. The most recent rehabilitation of the monument at the beginning of the 20th century did not address the weakness of the basilica along the N-S axis. Consequently, during the 1978 earthquake, the flexible untrimmed wooden floors and timber roofs of the galleries held but did not prevent the columns from conducting autonomously. The earthquake was registered as a divergence of the longitudinal walls and colonnades from the vertical axis, caused primarily by marginal shifting. After the 1978 earthquake, which aggravated the pre-existing static sensitivity of the structure, the basilica presented multiple masonry disorganizations caused by intense compressive or tensile strain. Masonry cracks and trichoid fissures were observed in nearly all the arches and windowsills of the northern main wall, the semi-dome of the sanctuary apse and the superstructure of the perimetric walls due to the thrust of the timber trusses of the central aisle's roof. Sectional masonry disorganizations and detachments of the external masonries at their junction corners were also observed and were particularly severe at the NE and SW corners (Raptis and Zombou, 2010). The main problem of the monuments remained the declination of the southern colonnade and northern external masonry from the vertical axis.

Subsequent analysis of the current state of the monument with respect to its behavior under seismic activity indicated that the non-partial or overall dilapidation of the basilica during the 1978 earthquake was due to the diaphragmatic function of the timber floors and roofs of the galleries. Because of these influences, the seismic stress was transferred to the west wall of the narthex and the east wall of the main aisle, both of which functioned as rigid walls (Penelis and Stylianidis 1998, 2001). In the framework of the current study, a finite element model of the temple was constructed. In this model, the initial higher walls over the North and South internal colonnades are represented. Two main eigenperiods at this construction phase are estimated along the North - South direction at 0.73sec and 0.47sec in the West - East direction.

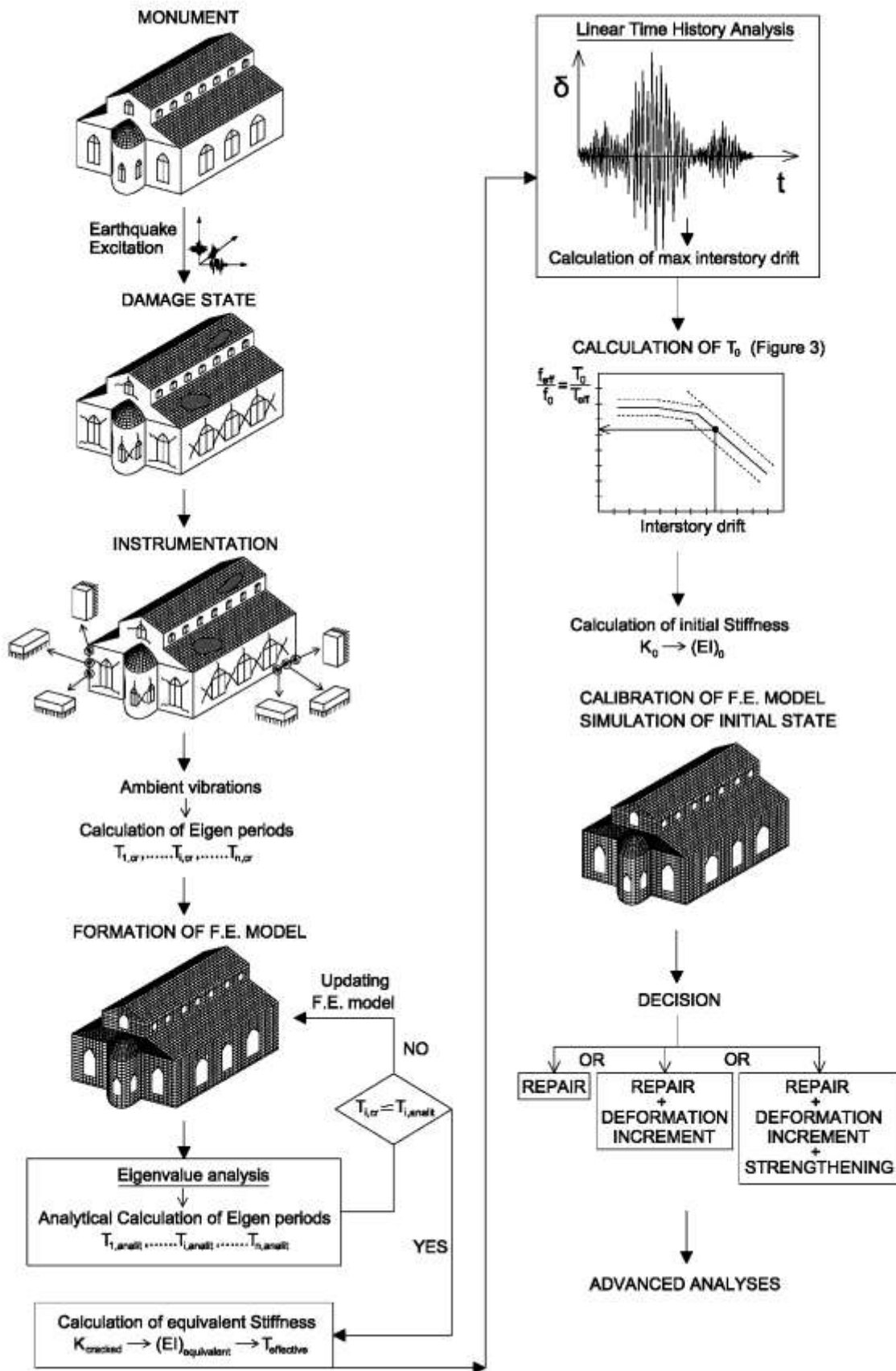


Figure 15. After-event method.

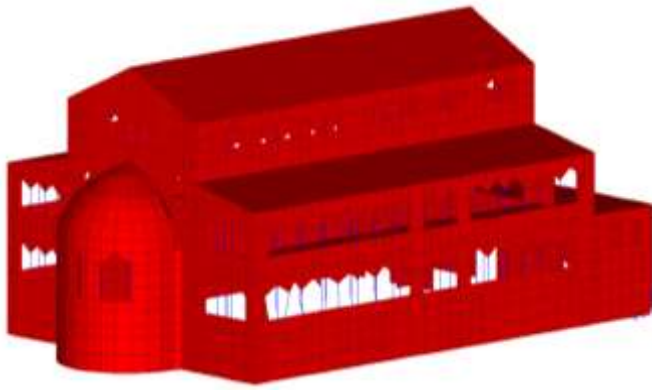
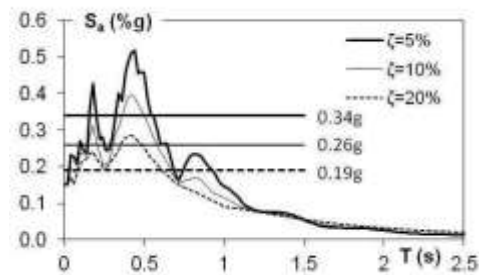
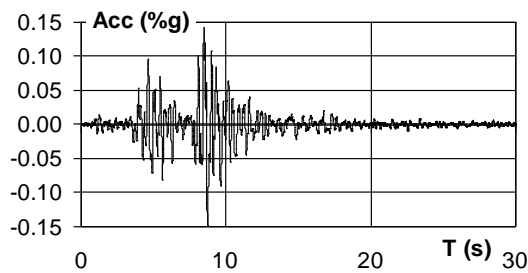


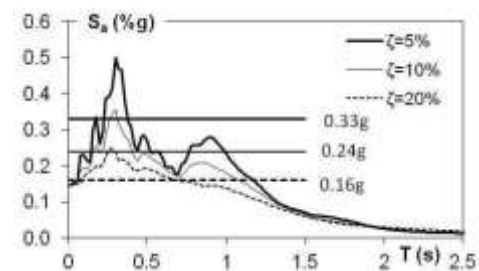
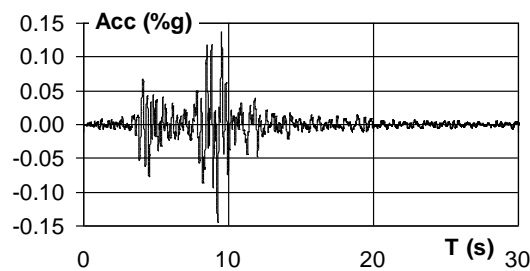
Figure 16. Left: North - East view of the model of the temple (Initial construction phase). Right: South - East view of the temple (Current period construction phase).

After the review of the earthquakes that happened in the area of Thessaloniki, it was found that three earthquakes that happened in 620 A.D. ($M=7.0$), 677 A.D. ($M=6.5$) and 700 A.D. ($M=6.6$) were the most important. It is believed that the middle higher part

of the temple fell after these earthquakes. The examination of the response of the temple to the earthquake that happened in 1978 in Stivos, close to Thessaloniki, follows in Figure 17. Two different equivalent dampings of 5% and 20% are used.



Accelerogram and response spectrum for the Thessaloniki Earthquake, 1978, $M_w=6.5$, Trans. Direction



Accelerogram and response spectrum for the Thessaloniki Earthquake, 1978, $M_w=6.5$, Long. Direction

Figure 17. Records of the Thessaloniki earthquake and resultant response spectra normalized (0.67 of the maximum value) for damping levels of 5%, 10% and 20%.

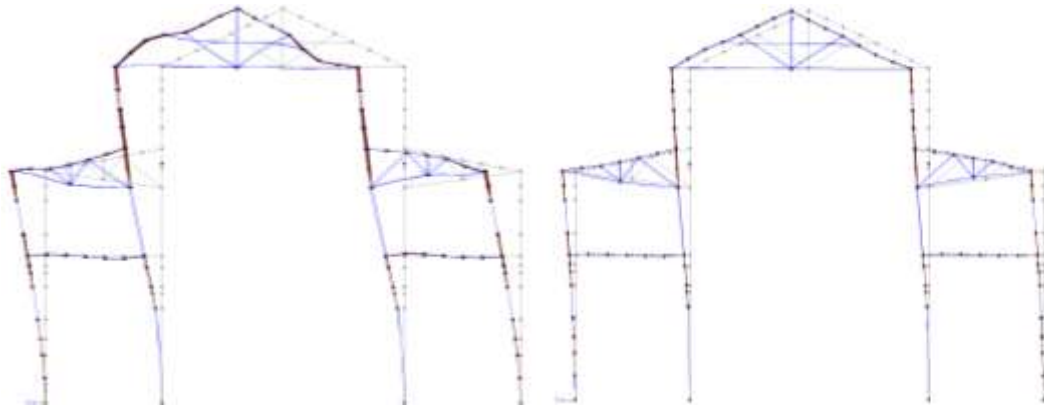


Figure 18. Deformation of the middle - section of the temple at 8.4sec of the earthquake time history, by considering 5% damping (left, max displ. 39mm) and 20% damping (right, max displ. 15mm). The monument was subjected to longitudinal direction time histories in the East - West axis and transverse direction time histories in the North - South axis.

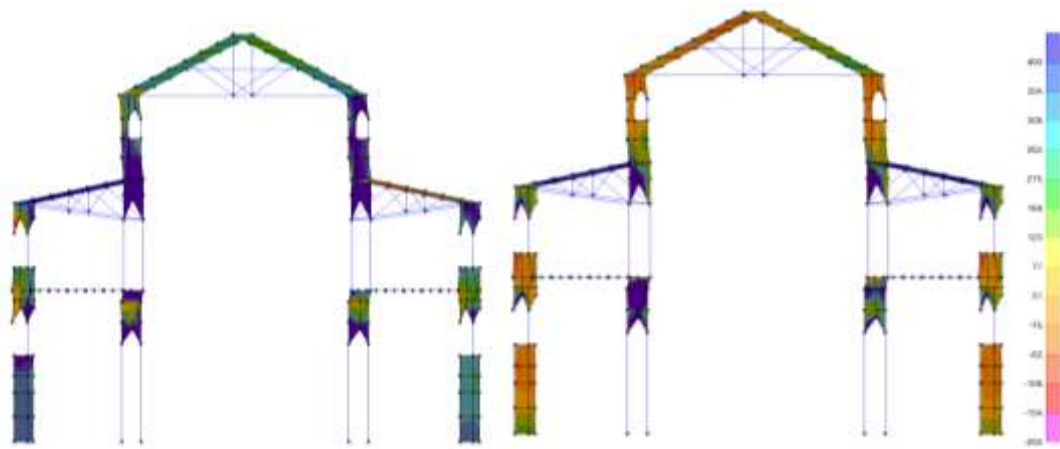


Figure 19. Tension stresses for 5% damping at left and 20% damping at right in kN/m^2 . The stress range is the same for both building sections (the right column refers to the same scale for both cases). In the left building section, there are tension stresses of 350kN/m^2 , while at the right section the tension stresses are of 170kN/m^2 .

By the use of the deformed sections that are shown, it is concluded that, when equivalent damping of 20% is considered, more reasonable deformations and loads are obtained. This in turn justifies the response of the basilica to strong earthquakes and the reason why the part of the wall that exceeded the roof fell and extended collapses were not observed. In Figures 18 and 19, the deformations and stresses are reduced by 50% when equivalent damping of 20% is used, in comparison with the consideration of 5% value.

8. CONCLUSIONS

Masonry monuments can develop “equivalent hysteretic” behavior when subjected to strong earthquakes. Additionally, a significant amount of the input seismic energy is absorbed and dissipated through the development of cracks, stiffness reduction and friction. “Equivalent ductility” could be considered in masonry monuments for reducing seismic loads either directly through a behaviour factor or indirectly through consideration of the

“equivalent damping” in advanced analysis methods. This conclusion is validated by considering: a) experimental tests run worldwide, b) the application of code provisions to the experimental data, c) inelastic analysis of plain masonry frames and d) earthquakes that occurred in the same area and that affected the same monument types. The aforementioned approaches were used to propose a methodology for estimating seismic loading in monuments, with the use of available data, records, analysis and recorded damages. The incentive behind this effort is a contribution to bridging the gap between the usually low analytically calculated strength of masonry monuments (during the evaluation of existing structures) with the actual response to strong earthquakes. In the current study, the comparisons and analyses that were conducted demonstrate that it is possible to determine rational seismic loads and interventions with documentation by estimating a reasonable behaviour factor or “equivalent damping” of the monuments. These conclusions are supported by a preliminary analysis

of the initial construction phase of a Byzantine Basilica and the limited collapses are justified by considering higher “equivalent damping”. In order to compose a code with appropriate regulations, as in the case of the seismic evaluation code for masonry monuments and other historical buildings, the exact behavior of these structures should be determined.

After the determination of the actual response of the masonry monuments to earthquakes, the code should then impose safety factors appropriate for materials and actions. The present research article provides data for appropriate consideration to the international existing and forthcoming codes.

REFERENCES

- Abrams, D.P. (1992) Strength and behaviour of unreinforced masonry elements. *Proceedings of the Tenth World Conference on Earthquake Engineering*. Madrid, Spain, pp. 3475-3480.
- Abrams, D.P. and Shah, N. (1992) Technical Report on Cyclic Load Testing of Unreinforced Masonry Walls. Advanced Construction Technology Center of University at Urbana-Champaign, Illinois
- Ahmad, N., Crowley, H., Pinho, R. and Ali, Q. (2010) Simplified Formulae for the Displacement Capacity, Energy Dissipation and Characteristic Vibration Period of Brick Masonry Buildings. *Proceedings of 8th Int. Masonry Conference in Dresden*, pp. 1385 – 1394.
- Beucke, K. and Kelly, J. (1985) Equivalent Linearization for Practical Hysteretic Systems. *Int. Journal of Non-Linear Mechanics*, Vol. 23(4), pp. 211 – 238.
- Bothara, J., Dhakal, R. and Mander, J. (2010) Seismic Performance of an Unreinforced Masonry Building: An Experimental Investigation. *Earthquake Engineering and Structural Dynamics*, Vol. 39(1), pp. 45 – 68.
- Calvi, M., Kingsley, G. and Magenes, G. (1996) Testing of Unreinforced Masonry Structures for Seismic Assessment. *Earthquake Spectra, Journal of Earthquake Engineering Research Institute*, Vol. 12(1), pp. 145-162.
- CEN. Eurocode 8-3 (2005) Design of structures for earthquake resistance – Part 3: Assessment and retrofitting of buildings, European Committee for Standardization.
- CEN. Eurocode 6-1-1 (2005) Design of masonry structures – Part 1-1: General rules for reinforced and unreinforced masonry structures, European Committee for Standardization.
- Corradi, M., Borri, A. and Vignoli A. (2002) Strengthening techniques tested on masonry structures struck by the Umbria-Marche earthquake of 1997-1998. *International Journal of Construction and Building Materials*, 16, pp. 229-239.
- Da Porto, F., Grendene, M. and Modena C. (2009) Estimation of load reduction factors for clay masonry walls. *Earthquake Engineering and Structural Dynamics*, 38, pp. 1155-1174.
- Elyamani, A and Roca, P (2018a) a review on the study of historical structures using integrated investigation activities for seismic safety assessment. Part I: dynamic investigation. *SCIENTIFIC CULTURE*, Vol. 4, No 1, pp. 1-27
- Elyamani, A and Roca, P (2018b) A review on the study of historical structures using integrated investigation activities for seismic safety assessment. Part II: model updating and seismic analysis. *SCIENTIFIC CULTURE*, Vol. 4, No 1, pp. 29-51
- Elyamani, A (2018c) Re-use Proposals and Structural Analysis of Historical Palaces in Egypt: The Case of Baron Empain Palace in Cairo., *SCIENTIFIC CULTURE*, Vol.4, No.1, 53-73.
- Ignatakis, C., Stylianidis, K. (2004) Mechanical Characteristics of Virgin and Strengthened Old Brick Masonry – Experimental Research. *International Journal of the British Masonry Society*, 17(1), pp. 9-17.
- Institute of Engineering Seismology & Earthquake Engineering (2008). The Koroni Earthquake of February 14, 2008. Report at: http://www.itsak.gr/uploads/news/earthquake_reports/Koroni_2008.pdf.
- Institute of Engineering Seismology & Earthquake Engineering (2008). The Achaia – Ilia Earthquake M=6.5, June 8, 2008. Report at: http://www.itsak.gr/uploads/news/earthquake_reports/AchaiaIlia/Achaia-Ilia_Jun2008_4thReport.pdf
- Institute of Engineering Seismology & Earthquake Engineering (ITSAK) & Institute of Geodynamics of NOA (2003) The Vartholomio Earthquake M=5.6 of 2 December 2002. Technical Chamber of Greece, ISBN 960-8369-01-0.
- Karakostas, Ch., Makarios, T., Lekidis, V., Salonikios, T., Sous, I., Makra, K., Anastasiadis, A., Klimis, N., Dimitriou, P., Margaris, B., Papaioannou, Ch., Theodulidis, N. and Savvaidis A. (2006) The Kythira (Greece) Earthquake of January 8. Preliminary Report on Strong Motion Data, Geotechnical and Structural Damage. EERI Learning from Earthquakes report, at: https://www.eeri.org/lfe/pdf/greece_kythira_ITSAK.pdf

- Karantoni, F.V., and Fardis, M.N. (1992) Computed versus observed seismic response and damage of masonry buildings. *Journal of Structural Engineering ASCE*, Vol. 118(7), pp. 1804-1821.
- Karantoni, F.V. and Bouckovalas, G. (1997) Description and analysis of building damage due to Pyrgos, Greece, earthquake. *Soil Dynamics and Earthquake Engineering*, 16, pp. 141-150.
- Karantoni, F.V. and Fardis, M.N. (2005) Damage to masonry buildings due to the Aegion (GR) 1995 earthquake. *Structural Studies, Repairs and Maintenance of Heritage Architecture*, IX, pp. 191-201.
- Magenes, G. and Calvi, G.M. (1997) In-plane Seismic Response of Brick Masonry Walls. *Earthquake Engineering and Structural Dynamics*, 26(11), pp. 1091-1112.
- Michel, C., Zapico, B., Lestuzzi, P., Molina, F. and Weber, F. (2011) Quantification of Fundamental Frequency Drop for Unreinforced Masonry Buildings from Dynamic Tests. *Earthquake Engineering and Structural Dynamics*, Vol. 40(11), pp. 1283 - 1296.
- Penelis G. - Stylianidis K. Structural Restoration of the Acheiropoietus Basilica in Thessaloniki. Journal "Κτίριο (Building), Scientific Edition A/1998, pp. 33-40, (in Greek).
- Penelis G. G. - Stylianidis C. K. Structural Restoration of the Acheiropoietus Basilica in Thessaloniki. Proceedings of the 2nd International Congress on Studies in Ancient Structures 2001, Istanbul, Turkey.
- Raptis K., Zombou - Asimi A. (2010) The consolidation and restoration project of Acheiropoietos Basilica in Thessaloniki. Proceedings of MONUBASIN 2010, Patras, Greece.
- Salonikios, T., Karakostas, C., Lekidis, V. and Anthoine, A. (2003) Comparative Inelastic Pushover Analysis of Masonry Frames. *Engineering Structures*, Vol. 25(12), pp. 1515 - 1523.
- Tomaževič, M. (2009) Shear resistance of masonry walls and Eurocode 6: shear versus tensile strength of masonry. *International Journal Materials and Structures*, 42, pp. 889-907.
- Tomazevic, M. and Weiss, P. (1994) Seismic Behavior of Plain and Reinforced Masonry Buildings. *Journal of Structural Engineering ASCE*, Vol. 120(2), pp. 323 - 338.
- Theodulidis, N., Kalogeras, I., Papazachos, C., Karastathis, V., Margaritis, B., Papaioannou, Ch. and Skarlatoudis, A. (2004). HEAD v.1.0: A unified Hellenic Accelerogram Database, *Seismolog. Res. Lett.* Vol. 75, #1.